27
19

DR-1951

MASTER

ORNL-4727
UC-80 – Reactor Technology

DEFORMATION AND RUPTURE BEHAVIOR OF LIGHT-WATER REACTOR FUEL CLADDING

D. O. Hobson
P. L. Rittenhouse

OAK RIDGE NATIONAL LABORATORY
operated by
UNION CARBIDE CORPORATION
for the
U.S. ATOMIC ENERGY COMMISSION

BLANK PAGE

BLANK PAGE

ORNL-4727

Contract No. W-7405-eng-26

METALS AND CERAMICS DIVISION

DEFORMATION AND RUPTURE BEHAVIOR OF LIGHT-WATER REACTOR FUEL CLADDING

D. O. Hobson and P. L. Rittenhouse

OCTOBER 1971

OAK RIDGE NATIONAL LABORATORY
Oak Ridge, Tennessee
operated by
UNION CARBIDE CORPORATION
for the
U.S. ATOMIC ENERGY COMMISSION

CONTENTS

DEFORMATION AND RUPTURE BEHAVIOR OF LIGHT-WATER REACTOR FUEL CLADDING

D. O. Hobson and P. L. Rittenhouse

ABSTRACT

The results of transient-temperature burst tests performed on Zircaloy cladding tubes are presented. These establish base-line criteria with reference to reactor loss-of-coolant accidents and materials parameters and provide a basis for comparisons among multirod tests, tests with irradiated cladding, and in-reactor experiments. This study delineates the maximum expansion to be expected from each combination of pressure and heating rate and shows, rigorously, the effect of wall thickness variation on expansion. In addition, the α-to-β transformation is shown to have a large effect on the strain and rupture behavior of the tubing.

INTRODUCTION

The design basis or maximum credible accident considered in the assessment of the safety of light-water reactor systems is the double-ended rupture of a large pipe in the primary system. More probable but less severe accidents of a similar type could result from incomplete breaks in large pipes or from the complete severance of smaller pipes. This whole spectrum of accidents, in both boiling- and pressurized-water reactors (BWR and PWR), is known as the loss-of-coolant accident (LOCA). The LOCA results simultaneously in rapid loss of system pressure, expulsion of the coolant, and subsequent heatup of the fuel rod cladding. Redistribution of energy stored in the fuel, released by fission product decay, and – at sufficiently high temperatures – liberated by reaction between the zirconium-alloy cladding and steam all furnish heat for the transient. Emergency cooling systems are provided to terminate this transient by backfilling the reactor core with water. It is important, in the analysis of the LOCA – in terms of both emergency cooling capability and the magnitude of fission product

BLANK PAGE

release to the reactor containment — to know how the cladding will react during the transient (e.g., swelling and rupture temperature). For this reason a study of the transient burst behavior of fuel rod cladding under conditions simulating the LOCA was undertaken.

Transient temperature tests were performed on single, unirradiated, BWR-size, Zircaloy-4 tubes at a variety of heating rates and internal pressures to establish base-line data with reference to LOCA and material parameters and to provide a basis for subsequent comparisons among data obtained in multirod tests, tests with irradiated cladding, and in-reactor experiments. The tests were run under closely controlled and monitored conditions of thermal environment, heating rate, inert atmosphere, and specimen condition to simulate many of the variables the fuel rods would experience in a LOCA. At the same time, a suppression of other variables (such as steam oxidation and mutual interference of tube swelling by adjacent tubes on standard lattice pitch) kept the scope of the multiparameter study within useful limits. Tests were run with internal pressures from 50 to 1000 psig (initial pressure at 600°F) and with nominal heating rates of 10, 25, 50, and 100°F/sec. We determined the amount of circumferential expansion, amount of wall thinning, rupture temperature, and physical appearance of the tubing for each combination of test conditions.

EXPERIMENTAL PROCEDURE

It was imperative to cover as wide a range of variables as possible within a workable framework of parameters. We limited the tests to two controlled independent variables (internal pressure and heating rate) and one monitored variable (wall thickness variation). The dependent variables were rupture temperature, time to rupture, circumferential and wall thickness strains, maximum internal pressure, and the physical appearance of the ruptured tubing.

In a real reactor environment during a LOCA most fuel rods would undergo a thermal transient completely surrounded by similar rods undergoing identical transients. Under such conditions there should be no net transfer of heat from any tube to any other tube at any given level in the reactor core. We simulated this condition by using radiant heating in conjunction with a furnace, power supply, and controller designed for rapid thermal transient work. All equipment was manufactured by R-I Controls Division, Research Inc., Minneapolis, Minnesota. The furnace was a Quad-Elliptical heating chamber with a 10-in. heated length powered by five parallel-wired, quartz-sheathed, tungsten-filament lamps rated at 2 kW each. The furnace could be overpowered under transient conditions to a rating of 28.5 kW total. Power was furnished by a Thermac, series 6000 supply rated at 100 A at 480 V. The heating rates were controlled by a model FGE 5110 Data-trak programmer.

A cross section of the heating chamber is shown in Fig. 1. The pressurized specimen tube was centered in the furnace and contained one of the heater lamps. Four guard heaters were positioned around the chamber, and each heater was surrounded by a Zircaloy tube of the same cross-sectional dimensions, taken from the same lot of tubing as the specimens. The tubing used in the base-line study was BWR size (0.563 in. OD by 0.032 in. wall, nominal) obtained from AMAX Specialty Metals.

Temperatures were measured with Chromel vs Alumel thermocouples, spot welded to the tubing with a 0.003-in. tantalum foil interposed as a reaction barrier. The foil successfully prevented reaction between the thermocouples and the Zircaloy up to the melting point of the thermocouples. Initially, three thermocouples were used. One, on the specimen tube, was read by the controller-power supply; another, situated adjacent to the first on the specimen tube, was recorded on a strip chart. The third monitored the temperature of one of the guard tubes. This last thermocouple was used for the first six runs and was discontinued when the temperature difference between the specimen tubes and the guard tube were found to average 33°F at rupture temperatures as high as 2550°F. Examination of the heating curves for the specimens and the guard tube showed that very little temperature difference occurred between the tubes during the transients, and, therefore, little net transfer of heat could have occurred. Figure 2 shows the temperature variation with time for one of the runs. From this observation, and

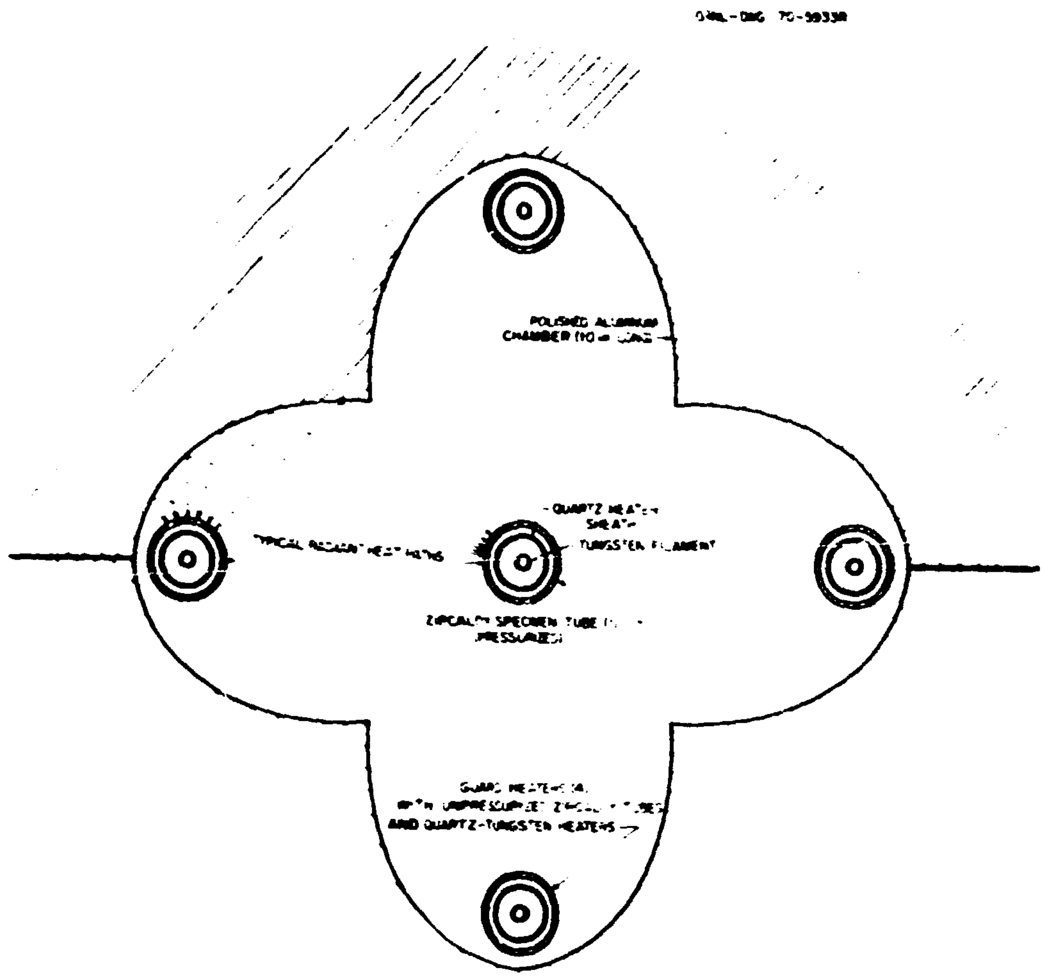

Fig. 1. Cross Section of the Radiant Heating Furnace Used to Generate Base-Line Data.

knowing the reflective characteristics of the furnace (uniform circumferential flux around the specimen and flux over the center 80% of the furnace chamber uniform within ±5%), one can infer that the thermal surroundings closely duplicated those postulated for a section of fuel rod in a LOCA. It should be emphasized that the thermal conditions characteristic of this experimental setup are more capable of producing the maximum tube expansion consistent with each set of test conditions than those achieved by induction heating, self-resistance heating, or muffle heating.

Tank argon of 99.99+% analyzed purity was used as both the pressurizing medium and the cover gas in all base-line experiments. A large plastic bag enclosing the entire furnace was alternately filled with argon through purge ports in the furnace and a separate line in the bag and evacuated to almost complete deflation by a vacuum pump. This cycle was repeated three or four times for each run, and the system

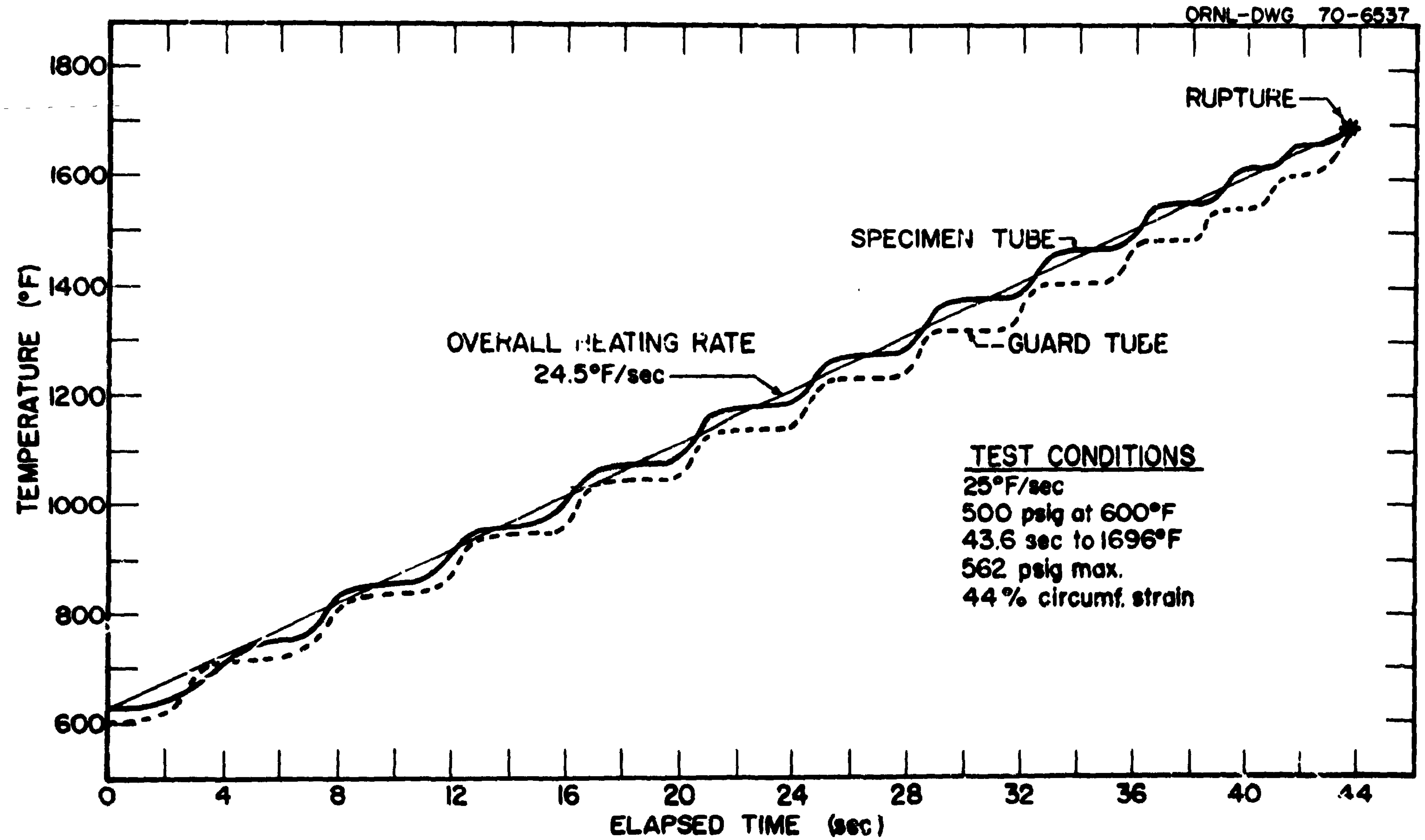

Fig. 2. Time Versus Temperature Curves Illustrating the Relative Heating Rates of the Specimen Tube and One Guard Tube During a Typical Test.

was sealed with the bag fully inflated. Small amounts of argon flow into both the furnace and the bag were maintained during the transient to counteract leakage. The specimen was alternately pressurized to greater than the desired test pressure and bled to atmospheric pressure four times before each run. The furnace (specimen and four guards) was preheated to 600°F, the pressure was adjusted to the desired value, and the specimen was valved off. Each test was initiated by switching the Data-trak on and, as the control sensor started up the transient ramp, switching on the various recorder drives. The tests were terminated just after rupture by cutting the power to the Thermac unit.

Circumferential strain was measured by wrapping a piece of Scotch "Magic" mending tape around the tube at the rupture, marking the tape at the rupture edges, removing the tape, and measuring the circumference from one edge of the rupture around to the other edge. To prevent stretching when it was removed from the tube, the tape was prestuck to a smooth surface several times to decrease the adhesion. Circumferential strain was defined as $100(C_F - W_R - C_0)/C_0$ where C_F = final circumference, W_R = width of rupture, and C_0 = original circumference.

Each tube was photographed to record the surface appearance and the shape and type of rupture, and the data were analyzed. Finally, each tube was sectioned through the region of maximum expansion and the maximum and minimum remaining wall thicknesses were measured. The minimum remaining wall thickness was defined to be at a point approximately 0.020 to 0.030 in. from the rupture edge.

RESULTS AND DISCUSSION

The data will be reported somewhat redundantly in this section in a series of figures that should both explain the results and allow ready comparison with data from other tests of this type.

Figure 3 is a plot of rupture temperature against time to rupture, with the data points characterized by initial internal pressure and maximum circumferential strain. The slopes of the four lines with their origin at 600°F represent the four heating rates employed in our testing, and the distribution of the data points around these lines

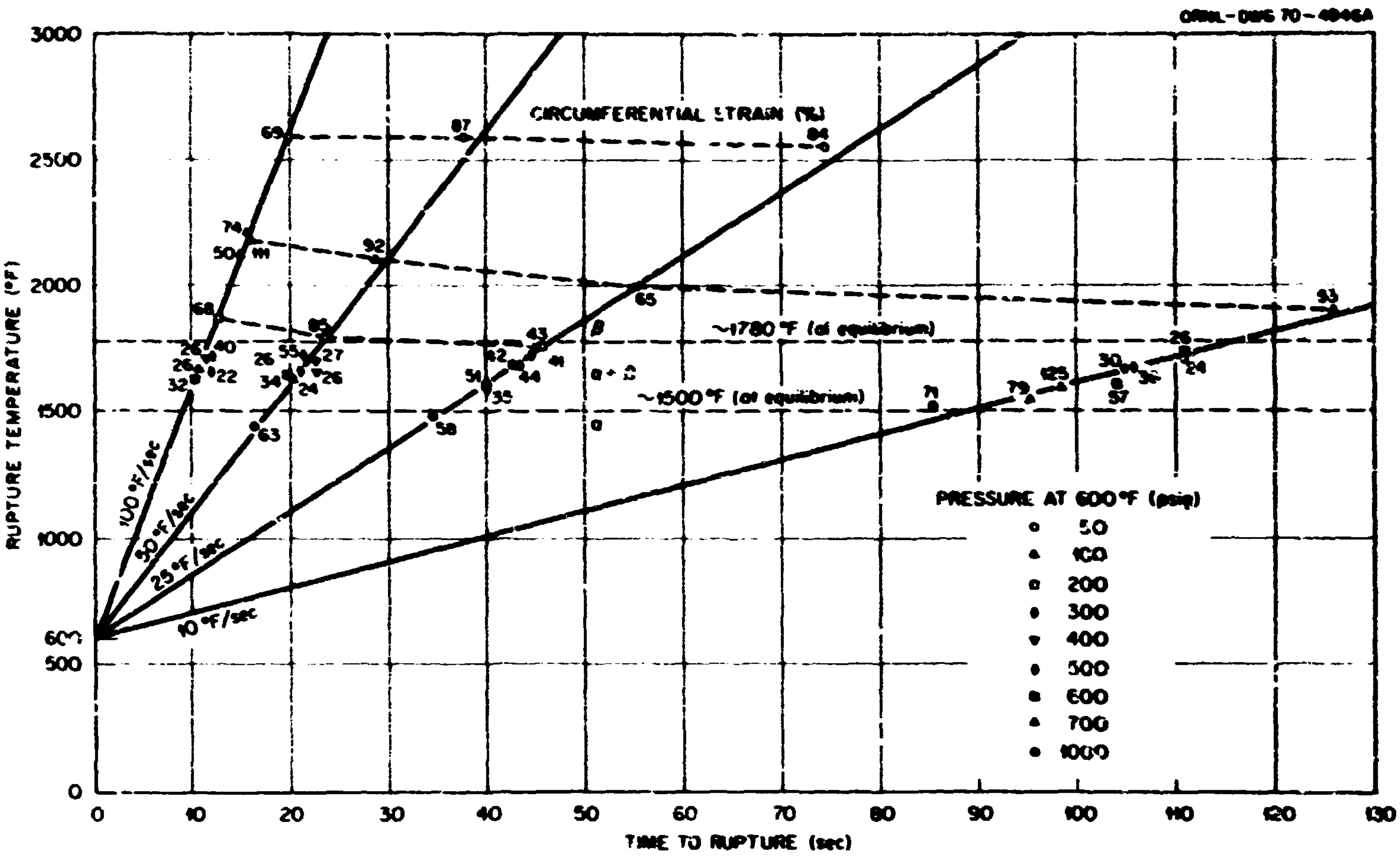

Fig. 3. Rupture Temperature Plotted Against Time to Rupture, with Data Points Characterized by Initial Pressure and Maximum Circumferential Strain.

indicates the accuracy of the test temperature control. The horizontal lines at 1500 and 1780°F represent the equilibrium transformation temperatures in Zircaloy. These temperatures are approximate in this case, since they are sensitive to alloy and impurity content and to heating rate. Their positions, however, separate the data into three interesting groupings. The points representing tests run at 50 and 100 psig and two of the points representing 200-psig tests show circumferential strains greater than 65%. These points all fall in the β, or body-centered cubic, phase of Zircaloy. The two points with 50 and 74% strain, tested at 100°F/sec and 100 psig, will be discussed later. The points grouped in the α + β region, with the exceptions of the tests run at 700 and 1000 psig and 10°F/sec, indicate ruptures occurred in the two-phase region with strains ranging from 22 to 57%. The remaining points, including the exceptions mentioned above, define ruptures that probably occurred in the single-phase α, and hexagonal close-packed, region. Here the strains have increased and range from

58 to 125%. Generally, specimens that exhibited low strains ruptured with smooth, often razor-sharp edges. The ruptures appeared to have blown out relatively violently and were preceded by very little uniform diametral expansion. In other words, all of the circumferential strain occurred in the region around the hole. The specimens with expansions greater than 65% all appeared to expand more uniformly. These observations agree quite well with the rupture temperatures; that is, whether the tubes ruptured in the single- or two-phase region. The α-to-β transformation in zirconium is a diffusionless, shear operation, and the shear can be directed by the applied stress. The relative amounts of α and β in the two-phase region vary with temperature so that, during a temperature transient through this region, one phase is continuously transforming to the other. This situation is conducive to rapid failure at the weakest point in the tube wall. The ability of the material to work harden while in the two-phase region should be small. However, if the pressure in the tube is low enough that rupture does not occur until the specimen has reached the single-phase β region, some work hardening could occur. This should prevent the rapid blowout that occurs in the two-phase region and should allow more uniform strain. Certainly the absence of the shear transformation would stabilize the mechanical properties of the tubing.

Figure 4 is a montage of photographs of the rupture areas of the tubes. The photographs are arrayed as a function of the heating rate and initial pressure. The dashed lines separate the specimens into the groups discussed above. The knife edges and the general lack of diametral swelling are quite obvious in the middle group of specimens whereas the lower and higher pressure specimens show much swelling and more jagged edges. The surface appearances are also different among the groups, with shiny surfaces on the medium- and high-pressure specimens and frosty or orange-peel textures on the low-pressure ones. The rupture openings were, in general, proportional to test pressure. The higher pressures tended to cause circumferential tearing at the four corners of the opening.

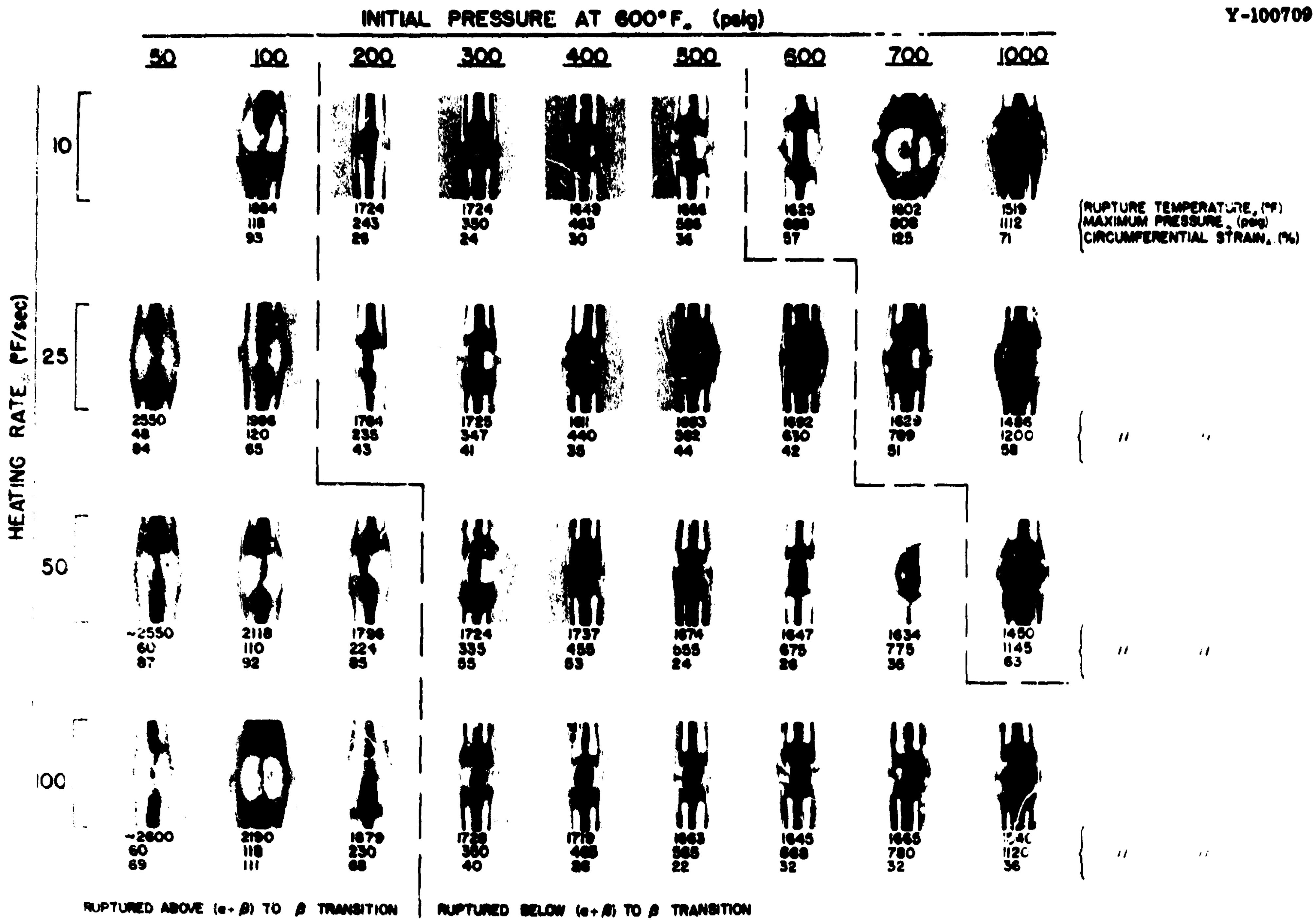

Fig. 4. Rupture Areas of the Tubes in the Base-Line Study.

The high-pressure specimens in the upper right corner were probably still in the single-phase α region when rupture occurred. The ability to work harden would have prevented nonuniform expansion and blowout.

When circumferential strain was plotted against maximum pressure (reached just before rupture), as shown in Fig. 5, a saddle occurred at 400 to 600 psig. These pressures correspond to rupture temperatures near the middle of the two-phase region. At both higher and lower pressures, corresponding to lower (α region) and higher (β region) temperatures respectively, the ductilities are greater.

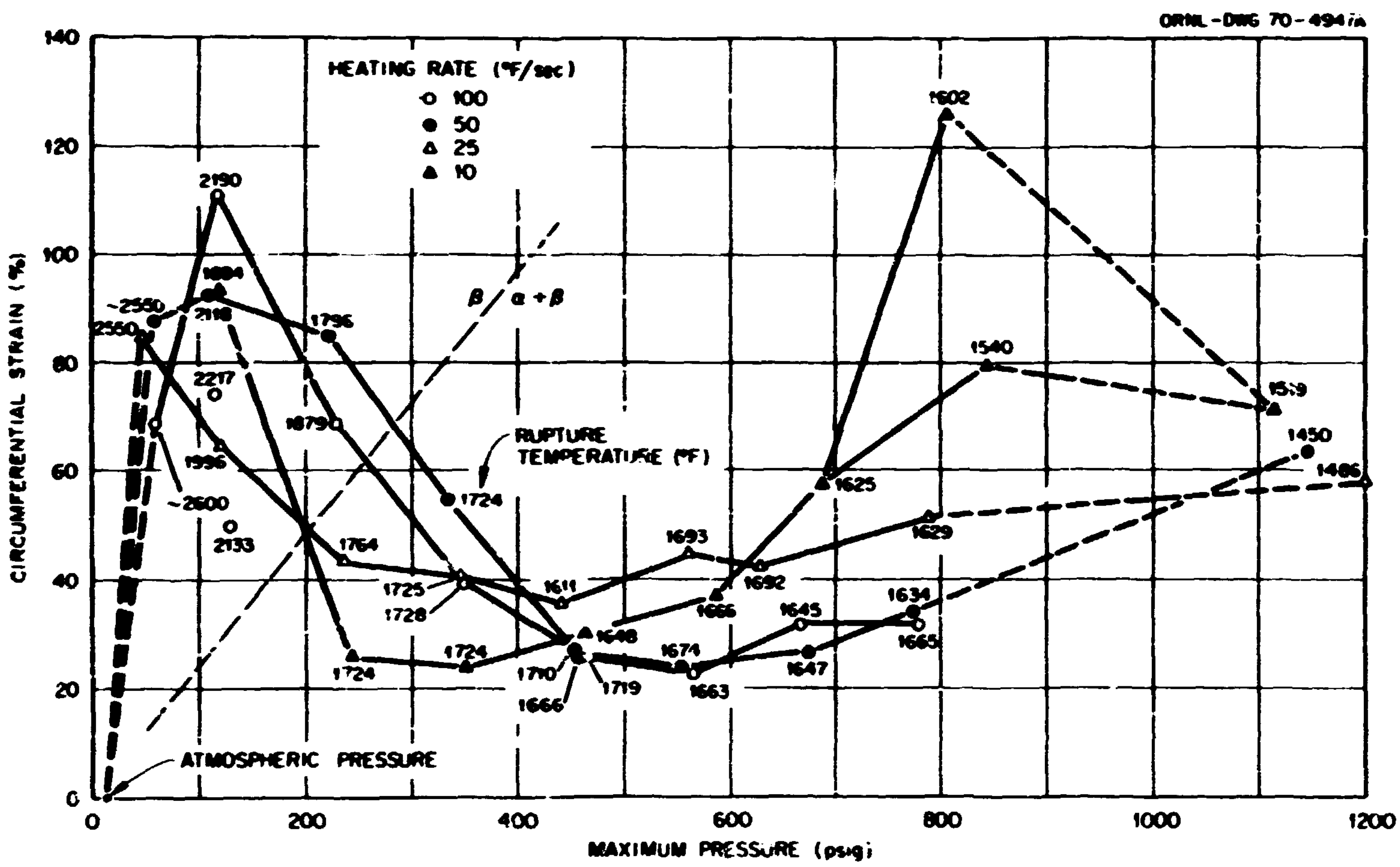

Fig. 5. Circumferential Strain Plotted Against Maximum Pressure. Base-line data illustrating the strain minimum that occurs at intermediate pressure levels.

The relationship between maximum pressure and burst temperature is shown in Fig. 6. The slope change at the ($\alpha + \beta$)-to-β transus is quite distinct. Of special interest are the points representing specimens pressurized to 100 psig initially and tested at four heating rates. These are found along the bottom middle of the graph and are identified by circumferential strains of 93, 65, 92, and 111%. These

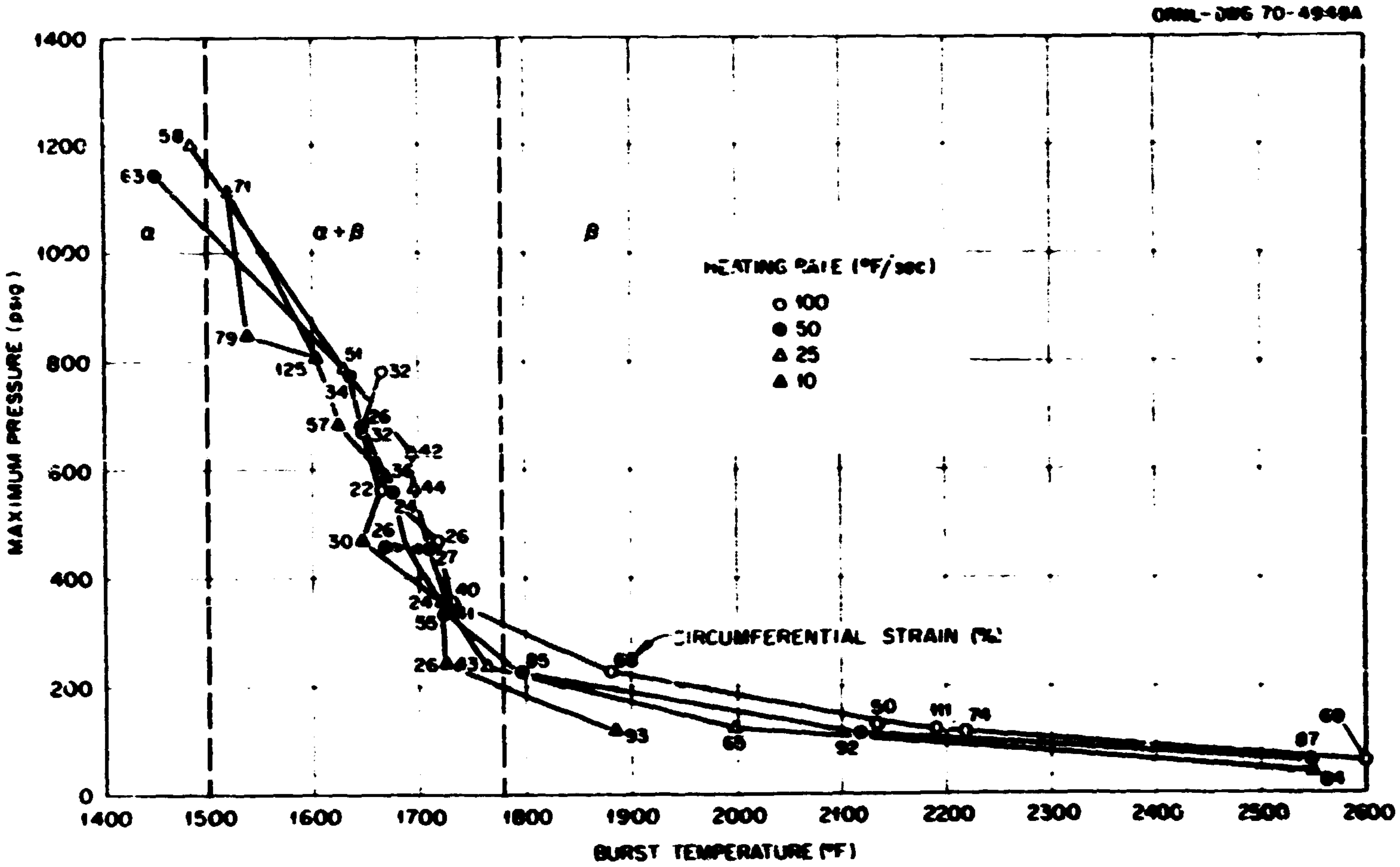

Fig. 6. Maximum Pressure Plotted Against Burst Temperature. Base-line data illustrating the inverse relationship between pressure and temperature.

four points demonstrate a strong effect of heating rate on the rupture temperature of the specimens. This effect is not found among the specimens that ruptured in the two-phase region. The times to rupture corresponding to the ductilities listed above were 126, 55, 29, and 16 sec, and the rupture temperatures were 1884, 1996, 2118, and 2190°F. Whether this phenomenon in the single-phase region is a creep effect or a time-at-temperature effect is probably not important. However, it is important to notice that such effects are found in the single-phase region and not in the two-phase. This indicates that the orderly cause-and-effect relationships among the variables in the single-phase region break down in the two-phase region. We conclude that the presence of the shear transformation during the transient through the two-phase region is the cause.

The effects of variations in initial wall thickness among the tubing specimens were quite noticeable in these tests. Normal ASTM specifications allow a 10% variation in wall thickness, approximately 0.003 in. In this study, wall thickness variations of up to 0.004 in.

were found around the circumferences of individual tubes. No tube with more than 0.002 in. variation produced circumferential strains greater than 74%. Nine of the 41 tubes tested had strains greater than 78%, and the wall thickness variations in these nine ranged from 0.0007 to 0.0019 in. The test in which a tube was run at 100°F/sec and 100 psig, and which gave 111% strain, was rerun with tubes that had 0.0027 and 0.0033 in. average wall thickness variation. These tubes had 74 and 50% circumferential strain, respectively. Even though the expansion and rupture were in the single-phase β region, where we postulate work hardening would oppose sudden blowout, the wall thickness variation was too great for uniform expansion. Four sets of test conditions involved duplicate or triplicate runs performed with specimens that had different amounts of wall thickness variation. Figure 7, a plot of circumferential strain against average wall thickness variation, illustrates the large decreases in ductility caused by the variation. Under the appropriate test conditions perfectly uniform tubing could have shown strains of 140% or greater.

A correlation was found between the position of the thinnest point in the original circumferences of the tubes and the direction of rupture. Figure 8 is a plot of wall thickness difference or variation against the angle that the rupture makes with the thin point. Out of the 41 tubes tested, 30 or 73% ruptured within 60° of the thin point. This correlation confirms the circumferential uniformity of the heating method used in these tests.

Figure 9, a plot of wall thickness against expansion, illustrates the results of post-test wall thickness measurements. As expected, the maximum post-test wall thickness values were smallest for specimens with the highest expansion: the tube wall must thin to allow circumferential expansion. The minimum wall thickness values were relatively constant. The least-squares straight line through those values omits the high data point, which was anomalous because of the difficulty of getting a true minimum thickness measurement on the severely "orange-peeled" wall.

The results shown in Fig. 9 are important with regard to the amount of embrittlement one would expect in a LOCA. In a thermal transient

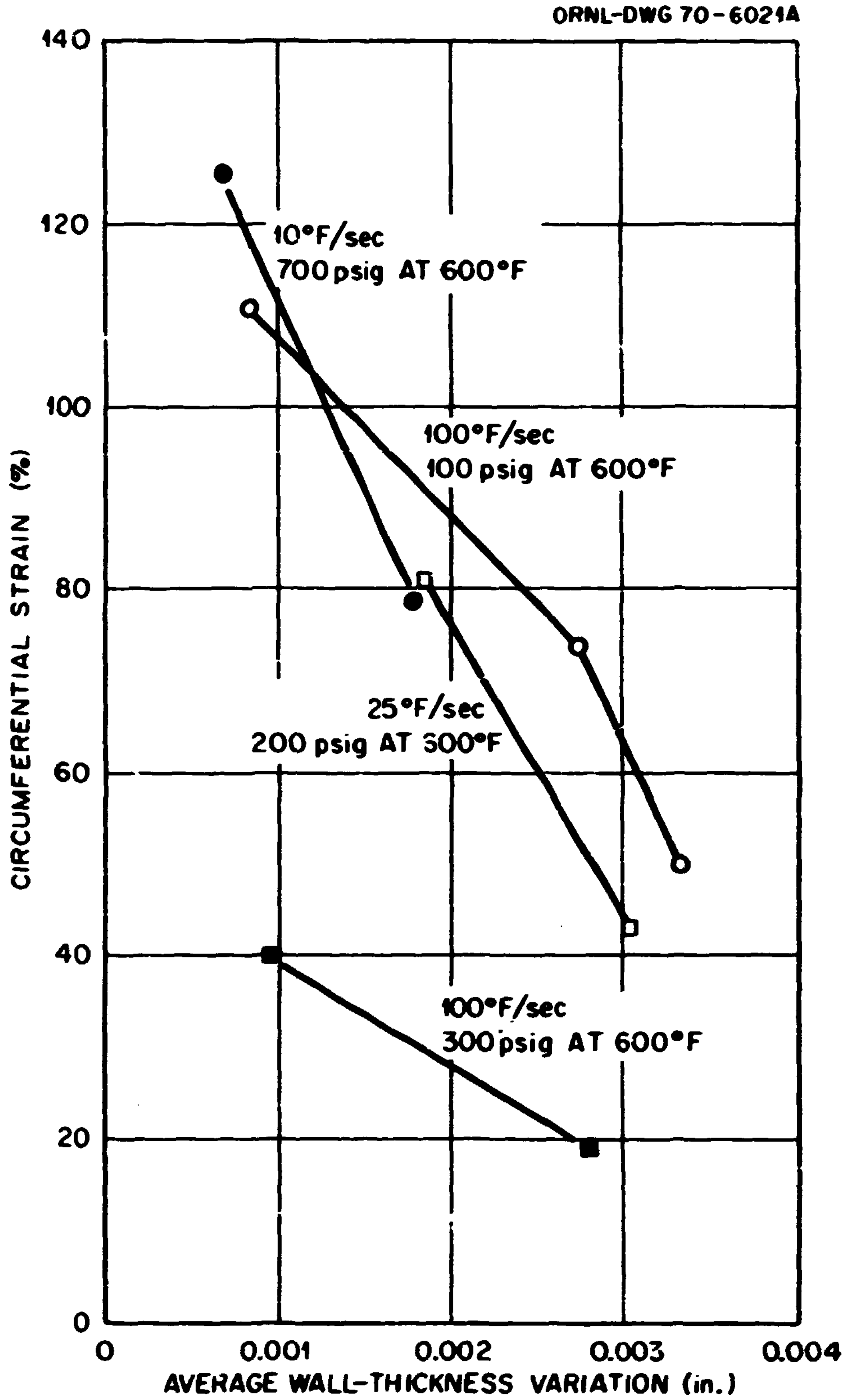

Fig. 7. Circumferential Strain Plotted Atainst Average Wall Thickness Variation, Illustrating the Large Decreases in Strain Caused by the Variations.

that takes place in steam, oxygen from the metal-water reaction will diffuse into the tube wall from one or both sides, depending upon whether rupture had occurred. Obviously, the thicker the wall, the longer the diffusion path and, therefore, the less the embrittlement for a given time-at-temperature history. Stated another way, the greater the expansion in a tube, the greater the amount of embrittlement for a given time-at-temperature history.

ORNL-DWG 70-6020R

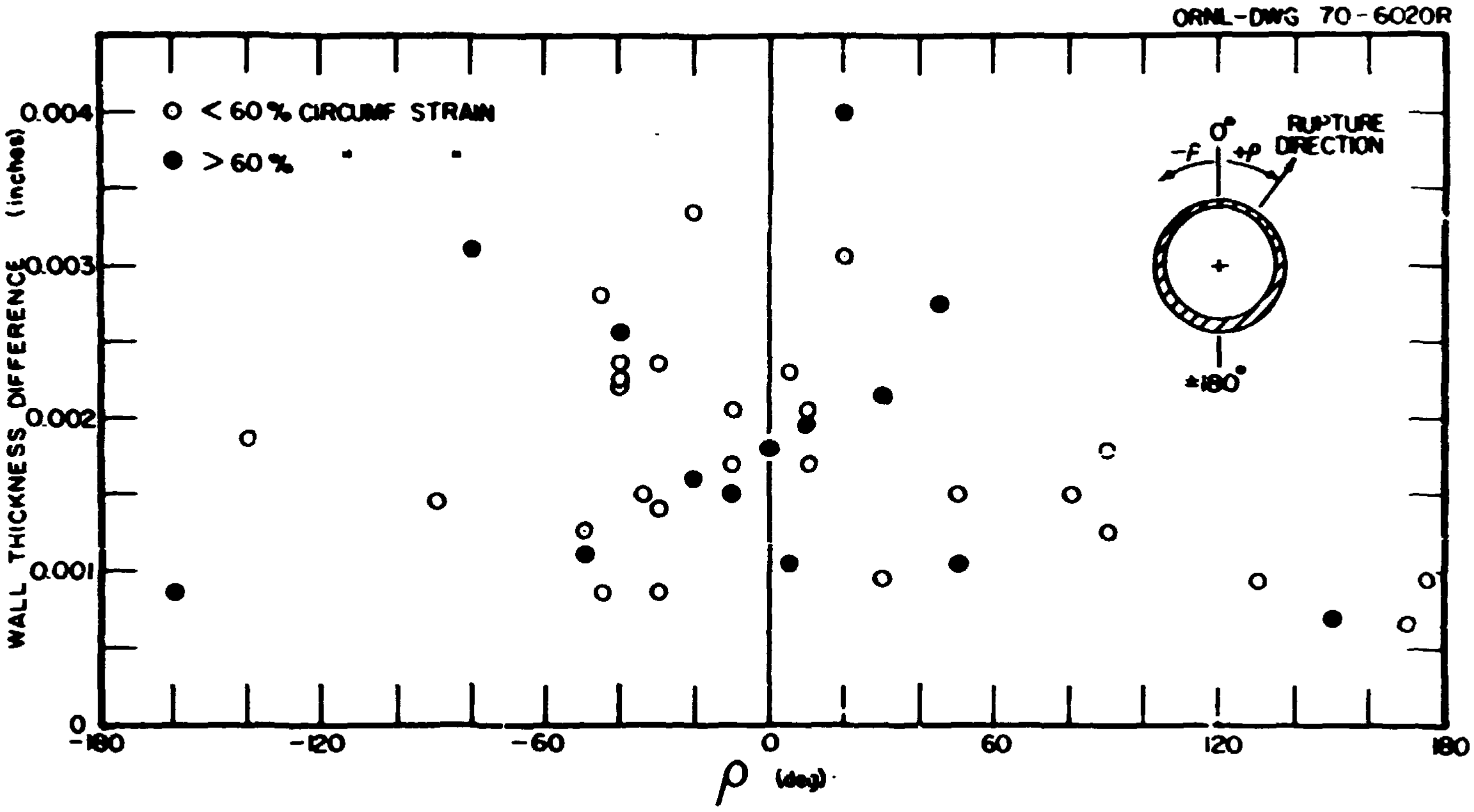

Fig. 8. Wall Thickness Variation Plotted Against the Angle, ρ, that the Rupture Makes with the Thin Point in the Tube Wall.

CONCLUSIONS

We obtained test results that delineate the behavior of Zircaloy tubing under carefully controlled heating rates and internal pressures. Circumferential expansion was very sensitive to rupture temperature, which, in turn, was a function of maximum internal pressure. Heating rate had a definite but less important effect on expansion. Expansion was minimized at internal pressures that caused rupture to occur in the two-phase $\alpha + \beta$ region, and we believe this is due to the lack of work hardening characteristic of deformation in that region. Heating rate had its greatest effect in the high-pressure region of the test design.

The major conclusion drawn from this study concerns the expansion minimum found with internal pressures between 400 and 600 psig. Such a minimum, with expansions of from 20 to 50%, could result in up to approximately 60% blockage of coolant channels in a multirod array; not a serious situation. Higher or lower pressures, corresponding to ruptures in the single-phase α or β regions, would produce greater amounts of channel blockage. Such effects have been seen in 13- and

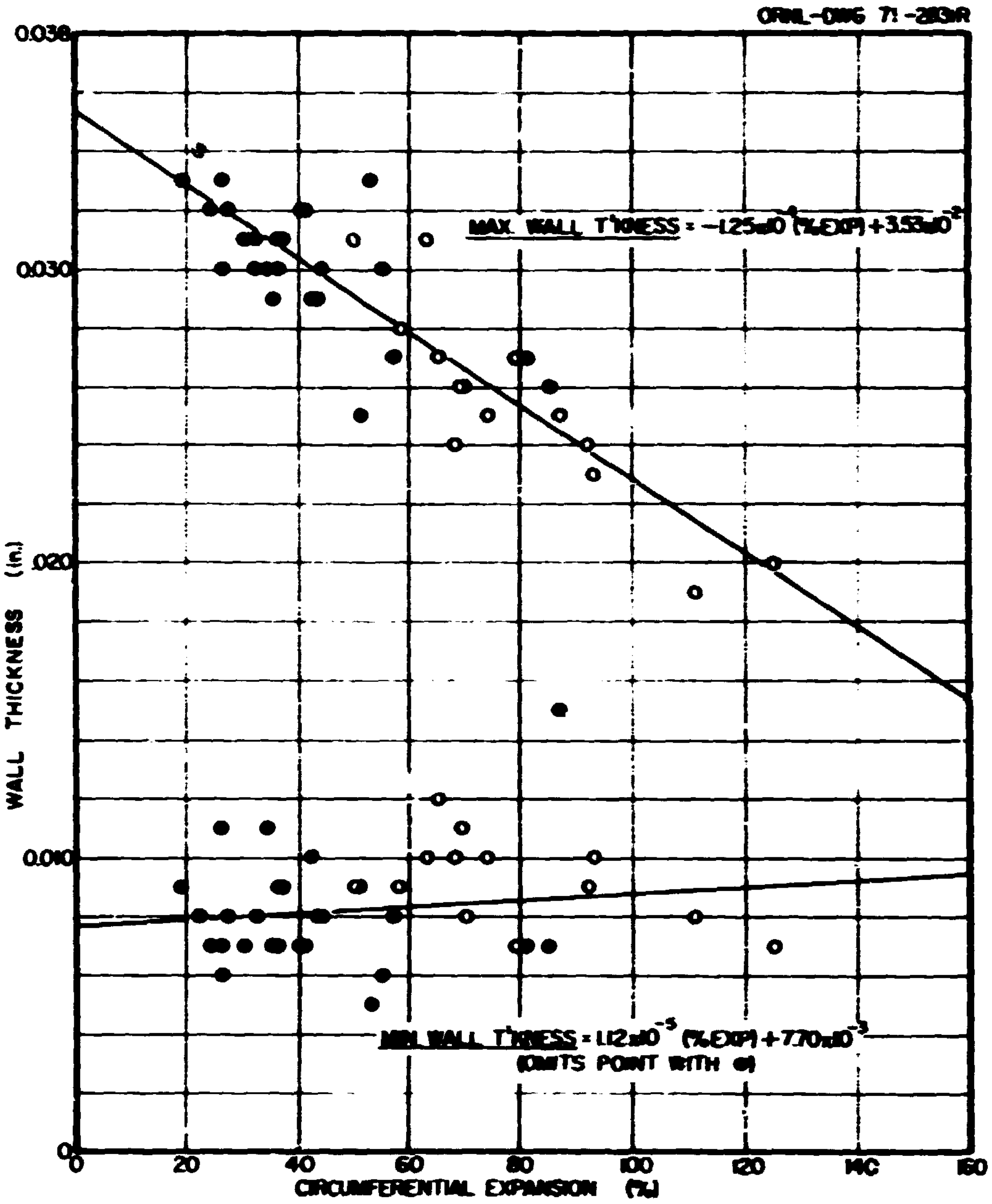

Fig. 9. Post-Test Wall Thickness Maxima and Minima Plotted Against Amount of Circumferential Expansion. Filled points indicate that rupture probably occurred in two-phase ($\alpha + \beta$) region. The point omitted from the least-squares fit of the bottom line had an anomalous wall thickness due to severe "orange peel" effect.

32-rod tests run at a variety of heating rates and internal pressures; the trends established in the base-line tests have been corroborated by the multirod results.

Wall thickness variation had a large effect on expansion, particularly under conditions where large amounts of expansion would be expected.

Large amounts of expansion produce two areas of concern. One is the effect of expansion on coolant channel blockage mentioned above. Coincident with this effect is that the wall thinning would increase susceptibility to oxygen diffusion into and embrittlement of the entire wall thickness.